

N 7 3 - 1 9 7 0 0

SPACE RESEARCH COORDINATION CENTER



CASE FILE
COPY

MEASUREMENTS OF RECOMBINATION
OF ELECTRONS WITH H_3^+ AND H_5^+ IONS

BY

M. T. LEU, MANFRED A. BIONDI AND R. JOHNSEN

SRCC REPORT NO. 184

UNIVERSITY OF PITTSBURGH
PITTSBURGH, PENNSYLVANIA

MARCH 1973

The Space Research Coordination Center, established in May, 1963, has the following functions: (1) it administers predoctoral and postdoctoral fellowships in space-related science and engineering programs; (2) it makes available, on application and after review, allocations to assist new faculty members in the Division of the Natural Sciences and the School of Engineering to initiate research programs or to permit established faculty members to do preliminary work on research ideas of a novel character; (3) in the Division of the Natural Sciences it makes an annual allocation of funds to the interdisciplinary Laboratory for Atmospheric and Space Sciences; (4) in the School of Engineering it makes a similar allocation of funds to the Department of Metallurgical and Materials Engineering and to the program in Engineering Systems Management of the Department of Industrial Engineering; and (5) in concert with the University's Knowledge Availability Systems Center, it seeks to assist in the orderly transfer of new space-generated knowledge in industrial application. The Center also issues periodic reports of space-oriented research and a comprehensive annual report.

The Center is supported by an Institutional Grant (NsG-416) from the National Aeronautics and Space Administration, strongly supplemented by grants from the A. W. Mellon Educational and Charitable Trust, the Maurice Falk Medical Fund, the Richard King Mellon Foundation and the Sarah Mellon Scaife Foundation. Much of the work described in SRCC reports is financed by other grants, made to individual faculty members.

Measurements of Recombination of Electrons with H_3^+ and
 H_5^+ Ions

The Physical Review

M. T. Leu, Manfred A. Biondi* and R. Johnsen

The University of Pittsburgh

Pittsburgh, Pennsylvania 15213

*Visiting Fellow, Joint Institute for Laboratory Astrophysics, University of Colorado.

Measurements of Recombination of Electrons

with H_3^+ and H_5^+ Ions *

M. T. Leu, Manfred A. Biondi [†] and R. Johnsen
Department of Physics
University of Pittsburgh
Pittsburgh, Pennsylvania 15213

Abstract

The electron-ion recombination coefficients for H_3^+ and H_5^+ ions have been determined by means of a microwave afterglow/mass spectrometer apparatus. Measurements of electron density decays in helium-hydrogen mixtures are correlated with the decay of mass-identified ion currents to the wall of the microwave cavity. At low partial pressures of hydrogen in the mixture, the ion H_3^+ dominates the ion composition and the ion wall current "tracks" the electron density decay curves. From recombination controlled electron density decay curves, the values $\alpha(H_3^+) = (2.9 \pm 0.3)$, (2.3 ± 0.3) , and $(2.0 \pm 0.2) \times 10^{-7} \text{ cm}^3/\text{sec}$, are obtained at 205, 300 and 450 K, respectively. At higher partial pressures of hydrogen and low temperatures, where H_5^+ is the dominant ion, the value $\alpha(H_5^+) = (3.6 \pm 1.0) \times 10^{-6} \text{ cm}^3/\text{sec}$ is obtained at 205 K. The implications of these results concerning ionization levels in the atmospheres of the outer planets and in the interstellar medium are discussed.

*This research has been supported, in part, by NASA (NGR 39-011-137).

[†]Visiting Fellow, Joint Institute for Laboratory Astrophysics, University of Colorado.

I. Introduction

Optical spectroscopy has been employed to detect molecular hydrogen as the principal neutral gas species in the atmospheres of Jupiter⁽¹⁾, Saturn⁽²⁾, Uranus and Neptune⁽³⁾, and in interstellar clouds.⁽⁴⁾ The principal steps in the formation of hydrogen plasmas in the planetary ionospheres and in the interstellar medium are thought to be photoionization of H₂ by the processes



followed by conversion of H₂⁺ and H⁺ ions to H₃⁺ ions by the fast reactions^(5,6)



and



The reaction (3) may be not important in the interstellar medium.

Theoretical models of Jupiter's atmosphere^(7,8,9) and of interstellar clouds^(10,11) have been proposed in which the recombination of electrons with H₃⁺ ions is the dominant loss process for these ions. In the absence of accurate measurements of their recombination coefficients,

the models so far have adopted estimated values.

The rate of recombination of H_3^+ ions with electrons is expected to vary with the temperature of the ions and of the electrons. In the regions of interest, the neutral gas and ion temperatures vary from as low as ~ 4 K in the interstellar medium to ~ 150 K in the upper atmosphere of Jupiter. The electron temperature is thought to be greater than the ion temperature by as much as several hundred degrees in the atmospheres of the outer planets.⁽¹²⁾ Thus, laboratory measurements should, if possible, cover an extensive range of ion and electron temperatures in order that the measured rates be applicable to all regions where electron-ion recombination of the ion H_3^+ is important.

The present experiment involves production of a plasma of H_3^+ (or H_5^+) ions and electrons in our microwave afterglow/mass spectrometer apparatus and measurement of the rates of decay of electron density and of mass-identified ion wall currents under recombination controlled conditions. From the curves of the electron density decay we determine the rates of electron-ion recombination at various temperatures under conditions such that the electron and ion temperatures are equal to the gas temperature; $T_e = T_i = T_{\text{gas}}$.

II. Apparatus and Method of Measurement

The apparatus and method of measurement used in the present studies has been described in detail a number of times^(13,14,15) and will be discussed only briefly here. Figure 1 is a simplified diagram of our experimental apparatus. Research grade hydrogen and ultrahigh-purity

helium acting as a buffer gas are admitted to the microwave cavity by means of an ultrahigh-vacuum gas-handling system. A plasma containing hydrogen ions and electrons is generated by means of a microwave pulse lasting 40 μ sec from a magnetron operating at a repetition rate of 10 sec⁻¹. The resonant frequency shifts, $\Delta\omega(t)$, of the microwave cavity are determined by noting the time of maximum reflection of a low energy probing signal of swept frequency. These measured frequency shifts are used to calculate the "microwave-averaged" electron density, $\bar{n}_{\mu w}(t)$, defined by

$$\bar{n}_{\mu w}(t) \equiv \frac{\int_{\text{vol}} n_e(\vec{r}, t) E_p^2(\vec{r}) dV}{\int_{\text{vol}} E_p^2(\vec{r}) dV} = C[1 + (\nu_{\text{eff}}/\omega)^2] \Delta\omega(t), \quad (4)$$

where $n_e(\vec{r}, t)$ is the electron density, $E_p(\vec{r})$ is the probing microwave electric field, C is a coefficient involving a group of physical constants, and ν_{eff} is the effective electron-helium collision frequency.⁽¹⁵⁾ The use of helium buffer gas at pressures approaching 20 Torr necessitates a $\sim 3 - 5\%$ correction of the electron densities⁽¹⁵⁾ determined from the frequency shifts compared to the low pressure case, $\nu_{\text{eff}} \ll \omega$.

A fraction of the ions which diffuse to the cavity wall and effuse through a small sampling hole enter a differentially pumped quadrupole mass spectrometer where they are mass identified. The ion counts at each afterglow time interval are coherently summed over many cycles by means of a multichannel analyzer operating in a multiscaling mode. In this manner, the decays of the positive ion wall currents are determined during the afterglow.

Under experimental conditions where only one ion species (H_3^+) predominates in the afterglow and electron-ion recombination is the only significant afterglow process (i.e. electron attachment, diffusion, and production processes are negligible) the electron density continuity equation simplifies to

$$\frac{\partial n_e}{\partial t} \approx -\alpha n_+ n_e \approx -\alpha n_e^2, \quad (5)$$

where α represents the two-body electron-ion recombination coefficient and we have set $n_e \approx n_+$ because of the near-neutrality of the afterglow plasma. The solution of this equation yields the well-known "recombination decay" form

$$\frac{1}{n_e(t)} = \frac{1}{n_e(0)} + \alpha t, \quad (6)$$

which indicates that the reciprocal of the electron density increases linearly with time, the slope of the curve yielding the recombination coefficient α .

In the cases of higher hydrogen pressures, however, two ions, H_3^+ and H_5^+ , are present and decay in an apparent chemical equilibrium with each other during the afterglow. It can be shown that the "recombination decay" form is still valid⁽¹³⁾ if α is replaced by an effective recombination coefficient α_{eff} given by

$$\alpha_{eff} = \frac{\alpha(H_3^+) + R\alpha(H_5^+)}{1 + R}, \quad (7)$$

where $\alpha(H_3^+)$ and $\alpha(H_5^+)$ are the recombination coefficients for H_3^+ and H_5^+ , respectively, and R is the ion concentration ratio, $[H_5^+]/[H_3^+]$.

By varying R by changing the hydrogen concentration the measured curve of α_{eff} vs. R can be used to evaluate $\alpha(H_3^+)$ and $\alpha(H_5^+)$ [the intercept at R = 0 is $\alpha(H_3^+)$; the limiting value for large R is $\alpha(H_5^+)$].

The analysis of the measured recombination decay curves to obtain the recombination coefficients involves consideration of the effects of ambipolar diffusion on the spatial distribution of the electrons within the cavity. As discussed previously⁽¹⁵⁾, tabulated correction factors⁽¹⁶⁾ are applied to the slopes of the $1/\bar{n}_{\mu W}$ vs. t curves to obtain the values of the recombination coefficients.

III. Results

A. H_3^+ Data

At helium pressures of $\sim 9 - 27$ Torr and hydrogen pressures of $\sim 5 - 13$ mTorr the principal afterglow ion is H_3^+ . This ion is evidently formed by the sequence; Penning ionization of H_2 by helium metastables, followed by rapid conversion of H_2^+ to H_3^+ by reaction (2).

An example of the data obtained at T = 300 K is shown in Fig. (2). In Fig. (2a) the experimental data follow a "recombination decay" (straight line) over a factor of 20 in electron density to a time of 10 msec, and then the curve turns upward due to diffusion effects. In Fig. (2b) the ion wall current curves are compared with the electron density decay curve. The dashed line through the H_3^+ curve is the $\bar{n}_{\mu W}$ curve renormalized. Although the H_3^+ curve does not "track" the electron density particularly

well in the early afterglow, H_3^+ is the only important ion throughout. While the ion H_5^+ is present the ratio of ion wall currents H_5^+/H_3^+ is approximately 10^{-3} , so that the effect of the ion H_5^+ on the determination of $\alpha(H_3^+)$ is negligible. After correction for ambipolar diffusion effects, the slope of the straight line in Fig. (2a) yields the value $\alpha(H_3^+) = 2.3 \times 10^{-7} \text{ cm}^3/\text{sec}$ at 300 K. The deduced values of $\alpha(H_3^+)$ vary by less than 5% as the helium pressure is varied between 14 and 27 Torr.

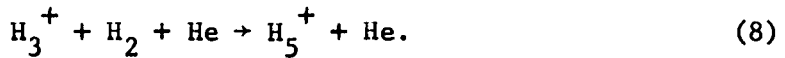
To study the H_3^+ recombination at $T = 450$ K, the microwave cavity was insulated and heated. An example of the data obtained at this temperature is shown in Fig. (3). Figure (3a) is the recombination plot; the data follow a straight line over a factor of 14 in electron density and then depart upward due to diffusion. In Fig. (3b) the only ion species observed, H_3^+ , is seen to more or less track the electron density curve. The corrected slope of the straight line in the plot of $1/n_{\mu W} vs. t$ yields the value $\alpha(H_3^+) = 2.0 \times 10^{-7} \text{ cm}^3/\text{sec}$ at 450 K. The deduced values vary by less than 5% as the helium pressure is varied from 17 to 20 Torr and the hydrogen pressure varied from 5.5 to 7.5 mTorr.

To study $\alpha(H_3^+)$ at $T = 205$ K, the cavity was immersed in a dry ice bath and the temperature measured by a copper-constantan thermocouple. The rate of formation of the ion H_5^+ showed a great increase at $T = 205$ K in comparison to the measurements at $T = 300$ K and $T = 450$ K. In Fig. (4b) are plotted the H_3^+ and H_5^+ ion wall currents and the relative electron density values. The dashed lines through the H_3^+ and H_5^+ ion curves are the electron density curves renormalized, indicating the "tracking" condition. In Fig. (4a) the electron density data

follow a recombination decay over a factor of 25 in electron density, indicating that the plasma is recombination controlled. The corrected slope of the straight line yields the effective recombination coefficient $\alpha_{\text{eff}} = 3.26 \times 10^{-7} \text{ cm}^3/\text{sec}$. After correcting for the presence of the ion H_5^+ by using $\alpha(H_5^+) = 3.6 \times 10^{-6} \text{ cm}^3/\text{sec}$ at $T = 205 \text{ K}$ (see next section), the recombination coefficient $\alpha(H_3^+) = 2.9 \times 10^{-7} \text{ cm}^3/\text{sec}$ is obtained at 205 K. As at the higher temperatures, the values of $\alpha(H_3^+)$ vary little (< 4%) as the helium pressure is varied from 8.6 to 16.6 Torr and the hydrogen pressure varied from 8 to 13 mTorr.

B. H_5^+ Data

By increasing the partial pressure of hydrogen, the ion composition is shifted from the dominance of H_3^+ to that of H_5^+ , presumably as a result of the increasing importance of the conversion reaction



As may be seen in Fig. (5b), the ion wall currents of H_5^+ and H_3^+ are observed to decay together, maintaining a constant ratio throughout most of the afterglow. Unfortunately, the tracking between ion wall currents and the electron density decay curve is not very good. Furthermore, there is a small concentration of the impurity ion $^{29+}$ present. It may be either the ion HN_2^+ or the ion HCO^+ because nitrogen and carbon monoxide are the major impurities in the helium buffer gas. From Fig. (5a) the corrected slope of the curve yields an effective recombination coefficient $\alpha_{\text{eff}} = 2.3 \times 10^{-6} \text{ cm}^3/\text{sec}$. Values of α_{eff} were obtained as a function of the H_5^+ and H_3^+ ion wall current ratio over the range

10^{-2} to 8.2 by varying the hydrogen concentration from 10^{-2} Torr to 0.6 Torr. The observed α_{eff} values are shown by the crosses in Fig.

(6). In order to compare the observed and predicted variations of α_{eff} , we have assumed that the measured ion wall current ratio is equal to the ion concentration ratio $[\text{H}_5^+]/[\text{H}_3^+]$. The solid curve represents the variation of α_{eff} with R predicted by Eq. (7). The values which give this degree of fit at $T = 205$ K are $\alpha(\text{H}_5^+) = 3.6 \times 10^{-6} \text{ cm}^3/\text{sec}$ and $\alpha(\text{H}_3^+) = 2.9 \times 10^{-7} \text{ cm}^3/\text{sec}$.

IV. Discussion and Conclusions

The uncertainties in the determinations of $\alpha(\text{H}_3^+)$ and $\alpha(\text{H}_5^+)$ are estimated in the following manner. Systematic errors in the resonant frequency measurements of the microwave cavity are less than 1%. The error in the afterglow time measurement (determined from a crystal oscillator time mark generator) is also less than 1%. The error in the electron density determinations due to collision frequency corrections of the frequency shift data is negligible. The principal errors in the determinations of $\alpha(\text{H}_3^+)$ and $\alpha(\text{H}_5^+)$ result from uncertainties in the diffusion correction factors.⁽¹⁶⁾ These uncertainties arise from imperfect knowledge of the initial spatial distribution of the electrons in the cavity and of the values of the ambipolar diffusion coefficients. This may lead to a $\sim 5\%$ error. Combining these uncertainties with that arising from the presence of the minority ion, the recombination coefficients of the ion H_3^+ are found to be (2.9 ± 0.3) , (2.3 ± 0.3) , $(2.0 \pm 0.2) \times 10^{-7} \text{ cm}^3/\text{sec}$ at 205 K, 300 K, 450 K, respectively.

The ion $^{29+}$, presumably HCO^+ , which has a recombination coefficient of $3.3 \times 10^{-7} \text{ cm}^3/\text{sec}$ at 205 K⁽¹⁷⁾, or N_2H^+ (with an estimated recombination coefficient of $\sim 3 \times 10^{-7} \text{ cm}^3/\text{sec}$), prevents us from reaching the asymptotic value at large R in our $\alpha(\text{H}_5^+)$ measurements. It appears that a 5-10% uncertainty may arise from this source. Considering the uncertainty in the determination of the ion wall current ratio $R = [\text{H}_5^+]/[\text{H}_3^+]$ and the presence of the impurity ion $^{29+}$, we expect a larger uncertainty in the H_5^+ recombination determination and assign the value $\alpha(\text{H}_5^+) = (3.6 \pm 1.0) \times 10^{-6} \text{ cm}^3/\text{sec}$ at 205 K.

The dependence of $\alpha(\text{H}_3^+)$ on temperature is shown in Fig. (7). The dashed line represents a $T^{-1/2}$ temperature dependence, which is a reasonable fit to the data. The theory of the direct dissociative recombination process⁽¹⁸⁾ suggests that the recombination rate for simple ions in a fixed distribution of vibrational states, should vary with the electron temperature as

$$\alpha(T_e) = c T_e^{-1/2}. \quad (9)$$

Our results indicate that this temperature dependence is obeyed, even though gas heating ($T_e = T_i = T_{\text{gas}}$) rather than selective heating of electrons ($T_e > T_i = T_{\text{gas}}$) was used. At these low temperatures (≤ 450 K), where the ions probably are predominantly in the ground vibrational state, the two types of temperature variation should lead to the same variation in recombination coefficient.

Several experiments had been performed to determine the electron loss in hydrogen. In 1949, Biondi and Brown⁽¹⁹⁾ used the microwave

cavity method without mass spectrometric analysis to determine the electron density decays in hydrogen. They found an electron-ion recombination coefficient of $2.5 \times 10^{-6} \text{ cm}^3/\text{sec}$ at 300 K, independent of the pressure between 3 and 12 Torr. At such high hydrogen pressures it is likely that the principal afterglow ion was H_5^+ , so that the measured value probably refers to $\alpha(\text{H}_5^+)$ and is in agreement with a reasonable extrapolation of the present results to 300 K.

Varnerin⁽²⁰⁾, using a microwave absorption afterglow technique, again without mass analysis, reported his determinations of recombination coefficients in hydrogen. They varied from a value of $3 \times 10^{-7} \text{ cm}^3/\text{sec}$ at hydrogen pressures of 1-3 Torr to a value of $2.5 \times 10^{-6} \text{ cm}^3/\text{sec}$ at pressures of 30-50 Torr. He paid more attention to purity, diffusing his hydrogen through hot palladium and baking his discharge tube thoroughly to outgas it. The pressure dependence of the recombination coefficient observed by Varnerin may reflect the changing concentrations of H_3^+ and H_5^+ as the principal afterglow ions as the pressure is changed. His value of $3 \times 10^{-7} \text{ cm}^3/\text{sec}$ at low pressures is about 30% higher than the present results for $\alpha(\text{H}_3^+)$ at $T = 300 \text{ K}$, while at high pressures his value of $2.5 \times 10^{-6} \text{ cm}^3/\text{sec}$ is also in reasonable agreement with an extrapolation of our $\alpha(\text{H}_5^+)$ value to 300 K.

Persson and Brown⁽²¹⁾ used intense microwave discharges in a microwave afterglow study of hydrogen and found that higher-mode ambipolar diffusion loss accounted fully for the observed electron concentration decays. The electron-ion recombination coefficient in these studies was inferred to be less than $3 \times 10^{-8} \text{ cm}^3/\text{sec}$. The measured ambipolar diffusion coefficient yielded a reduced ion mobility, $\mu_o = 16.6 \text{ cm}^2/\text{V sec}$, which is in excellent agreement with the measured

mobility of mass-identified H^+ ions.⁽²²⁾ Thus, in these studies H^+ was evidently the ion produced by the intense discharge and may have been the principal afterglow ion (although we do not understand why significant conversion of H^+ to H_3^+ via reaction (3) did not occur on the time scale of their afterglow measurements). With the atomic ion H^+ , significant recombination loss is excluded, and their results are compatible with the other studies.

One may compare our results with measured values⁽¹⁸⁾ of electron-ion recombination coefficients for ions such as N_2^+ , $N_2^+ \cdot N_2$, $O_2^+ \cdot O_2$, NO^+ , and $NO^+ \cdot NO$. The recombination coefficient for H_3^+ ($\sim 10^{-7} \text{ cm}^3/\text{sec}$) is comparable in magnitude to that for $\alpha(N_2^+)$, $\alpha(O_2^+)$, and $\alpha(NO^+)$ while the coefficient for $H_5^+ = (H_3^+ \cdot H_2)$ ($\sim 10^{-6} \text{ cm}^3/\text{sec}$) is comparable in magnitude to that for $(N_2^+ \cdot N_2)$, $(O_2^+ \cdot O_2)$, and $(NO^+ \cdot NO)$. The substantially different recombination coefficients for monomer ions and "dimer" ions may suggest that the recombination coefficient is related to the complexity of the ions, i.e. increases with the number of internal degrees of freedom of ions.

Finally, by using the $T^{-1/2}$ temperature dependence predicted theoretically for the direct dissociative process and observed in our experiments for simple ions at temperatures where the molecular ions are principally in their ground vibrational state, a value of $\alpha(H_3^+) \sim 4 \times 10^{-7} \text{ cm}^3/\text{sec}$ is expected at the ionospheric temperature of the outer planets ($\sim 100 \text{ K}$) and a value of $\alpha(H_3^+) \sim 2 \times 10^{-6} \text{ cm}^3/\text{sec}$ at the temperature of the interstellar medium ($\sim 4 \text{ K}$). If the indirect dissociative process occurs for H_3^+ , an even stronger inverse temperature dependence^(18,23) is to be expected at low temperatures, leading to even larger values of

$\alpha(H_3^+)$. Thus, those model calculations of the Jovian ionosphere assuming values of electron-ion recombination of the order^(8,9) of $\sim 10^{-8} \text{ cm}^3/\text{sec}$ for H_3^+ and H_5^+ require major revision. Similarly, calculations of polyatomic molecule formation in interstellar clouds⁽²⁴⁾ which use room temperature values of $\alpha(H_3^+)$ should also be modified.

References

1. C. C. Kiess, C. H. Corliss, and H. K. Kiess, *Astrophys. J.* 132, 221 (1960).
2. G. Munch and H. Spinrad, *Mem. Soc. Roy. Liege*, 7, 541 (1963).
3. G. Herzberg, *Astrophys. J.* 115, 337 (1952).
4. G. R. Carruthers, *Astrophys. J.* 161, L81 (1970).
5. R. N. Neynaber and S. M. Trujillo, *Phys. Rev.* 167, 63 (1968).
6. T. M. Miller, J. T. Mosley, D. W. Martin, and E. W. McDaniel, *Phys. Rev.* 173, 115 (1968).
7. S. H. Gross and S. I. Rasool, *ICARUS* 3, 311 (1964).
8. D. M. Hunten, *J. Atmos. Sci.* 26, 826 (1969).
9. S. S. Prasen and L. A. Capone, *ICARUS* 15, 45 (1971).
10. P. M. Solomon and M. W. Werner, *Astrophys. J.* 165, 41 (1971).
11. P. Thaddeus, *Astrophys. J.* 173, 317 (1972).
12. M. B. McElroy, *private communication* (1972).
13. C. S. Weller and M. A. Biondi, *Phys. Rev.* 172, 198 (1968).
14. F. J. Mehr and M. A. Biondi, *Phys. Rev.* 181, 264 (1969).
15. M. T. Leu, M. A. Biondi, and R. Johnsen, *Phys. Rev. A*7, 292 (1973).
16. L. Frommhold and M. A. Biondi, *Ann. Phys. (N.Y.)* 48, 407 (1968).
17. M. T. Leu, M. A. Biondi, and R. Johnsen, *Phys. Rev. (the next paper, this issue)*.
18. J. N. Bardsley and M. A. Biondi, "Dissociative Recombination" in *Advances in Atomic and Molecular Physics*, Vol. 6, edited by D. R. Bates, Academic Press, New York (1970).
19. M. A. Biondi and S. C. Brown, *Phys. Rev.* 76, 1697 (1949).
20. L. J. Varnerin, *Phys. Rev.* 84, 563 (1951).
21. K. B. Persson and S. C. Brown, *Phys. Rev.* 100, 729 (1955).
22. D. L. Albritton, T. M. Miller, D. W. Martin, and E. W. McDaniel *Phys. Rev.* 171, 94 (1968).

23. J. N. Bardsley, J. Phys. B. 1, 349, 365 (1968).
24. W. Klemperer, private communication, (1973).

Figure Captions

- Fig. 1.** Microwave afterglow apparatus employing differentially pumped quadrupole mass spectrometer to monitor the currents of various ions diffusing to the cavity walls (see text).
- Fig. 2.** (a) "Recombination plot" of electron density decay at 300 K.
 (b) Comparison of H_3^+ ion wall current and electron density decays.
- Fig. 3.** (a) "Recombination plot" of electron density decay at 450 K.
 (b) Comparison of H_3^+ ion wall current and electron density decay.
- Fig. 4.** (a) "Recombination plot" of electron density decay under effective recombination coefficient conditions at 205 K (see text).
 (b) Comparison of electron density and ion wall current decays under conditions where the ions H_3^+ and H_5^+ decay in apparent equilibrium. The dashed lines through the H_3^+ and H_5^+ data are scaled values of the electron density normalized to the curves at 2 msec.
- Fig. 5.** (a) "Recombination plot" of electron density decay under effective recombination coefficient conditions at 205 K. (see text).
 (b) Comparison of electron density and ion wall current decays under conditions where the ions H_5^+ and H_3^+ decay in apparent equilibrium and a small amount of the ion $^{29}+$ is noted. The dashed line through the H_5^+ data are scaled values of the electron density normalized to the curve at 2 msec.
- Fig. 6.** The effective recombination coefficient, α_{eff} , for different $[H_5^+]/[H_3^+]$ wall current ratios (measured at 2 msec in the afterglow. The solid line is a fit of the data to Eq. (7).
- Fig. 7.** Electron-ion recombination coefficient for H_3^+ at $T = 205, 300,$ and 450 K.

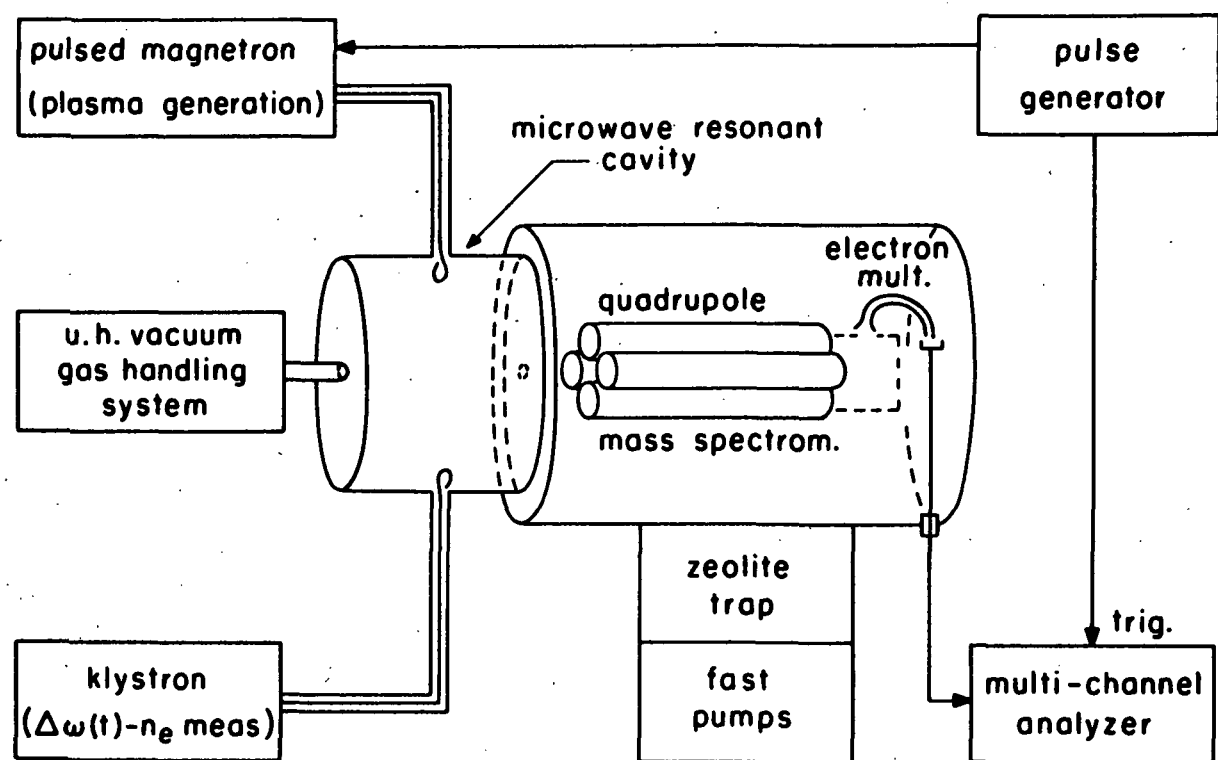


Figure 1

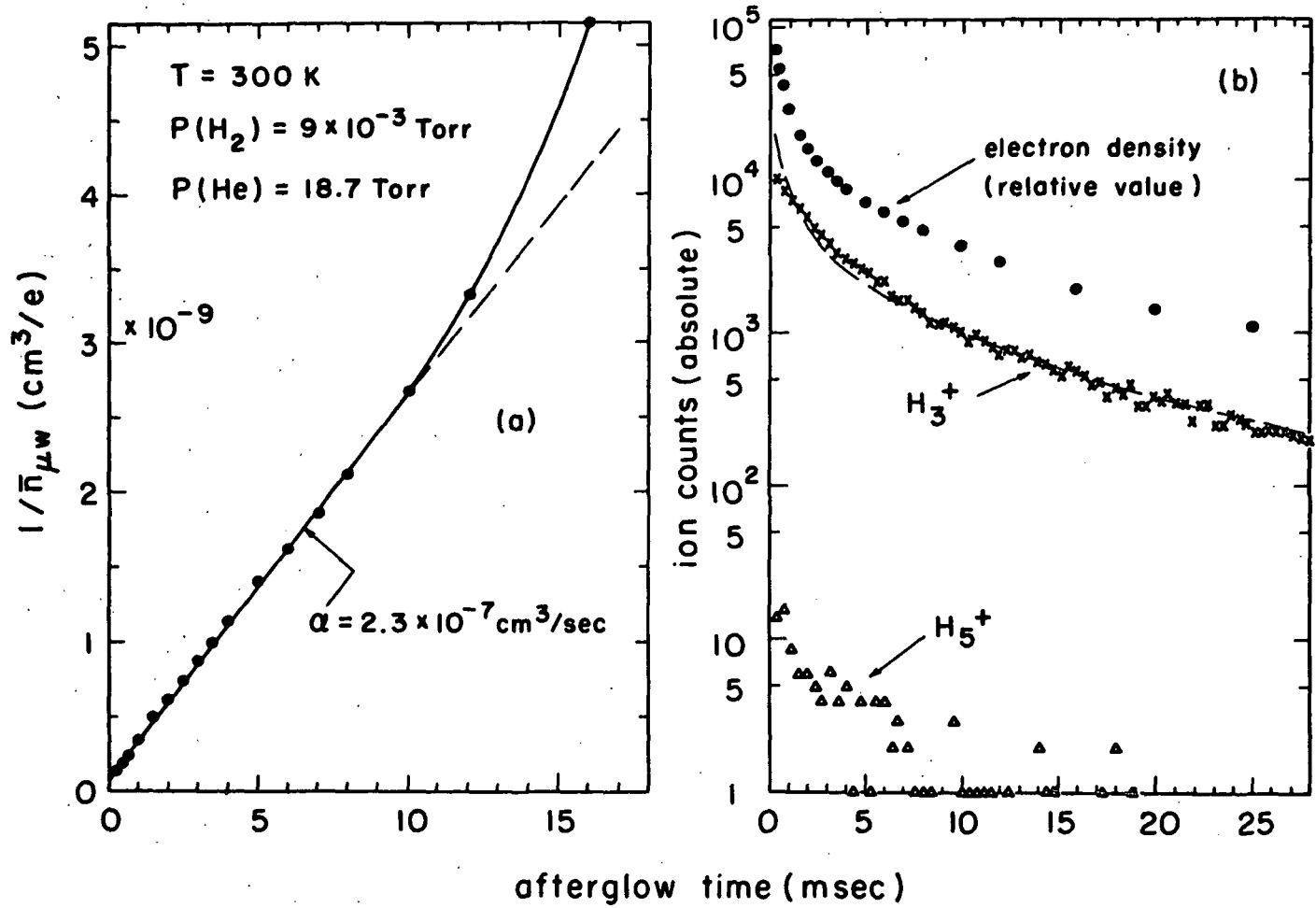


Figure 2

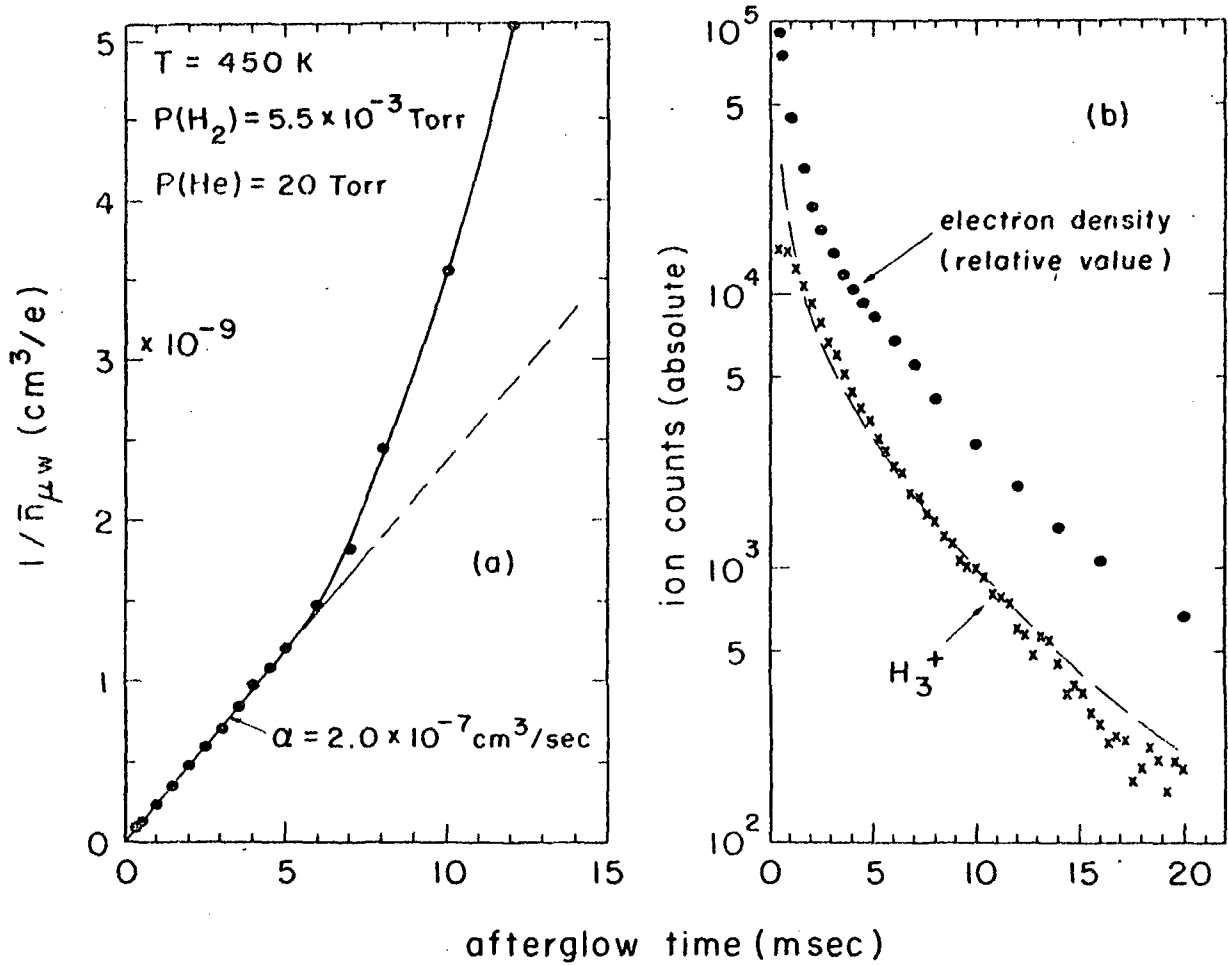


Figure 3

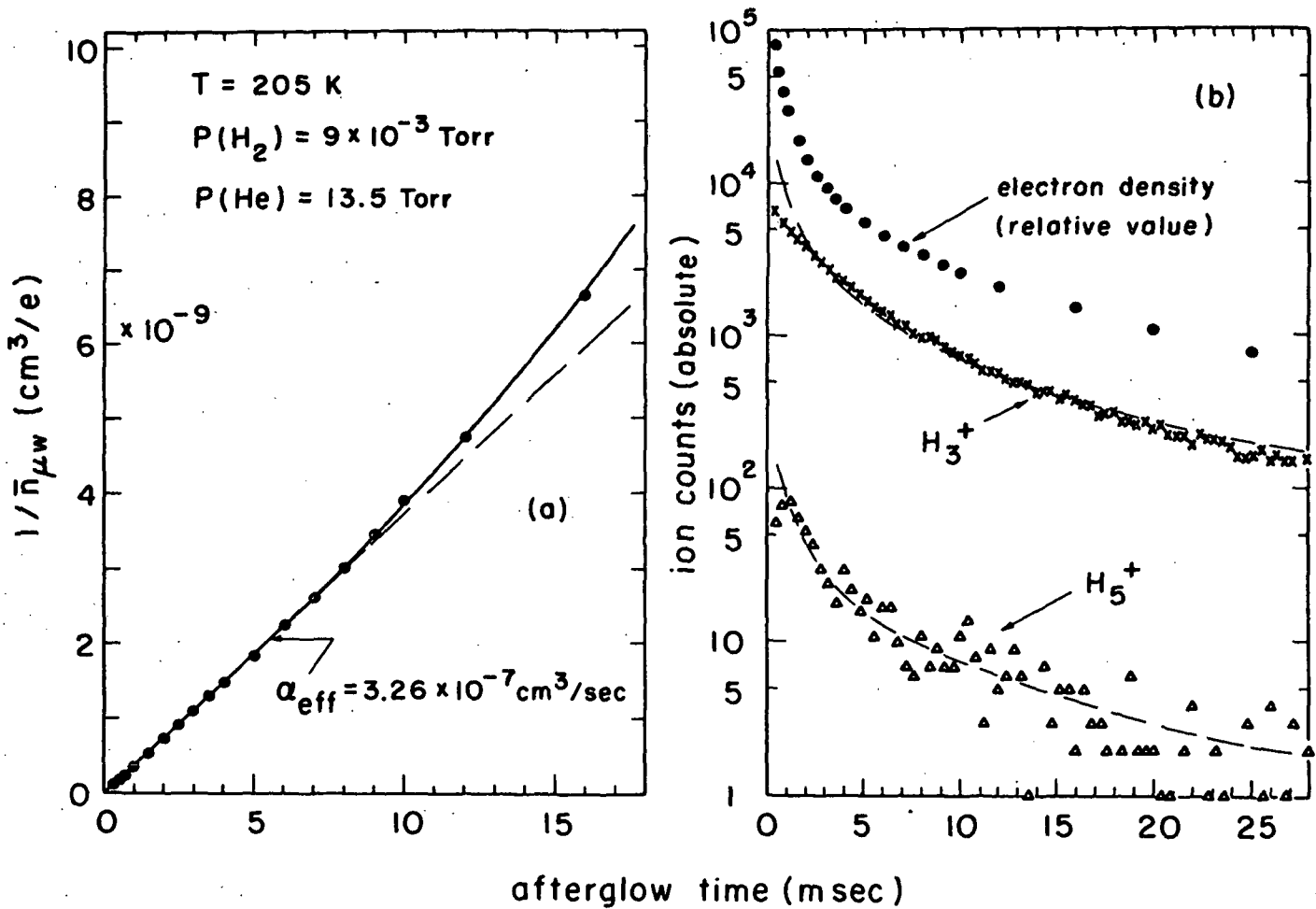


Figure 4

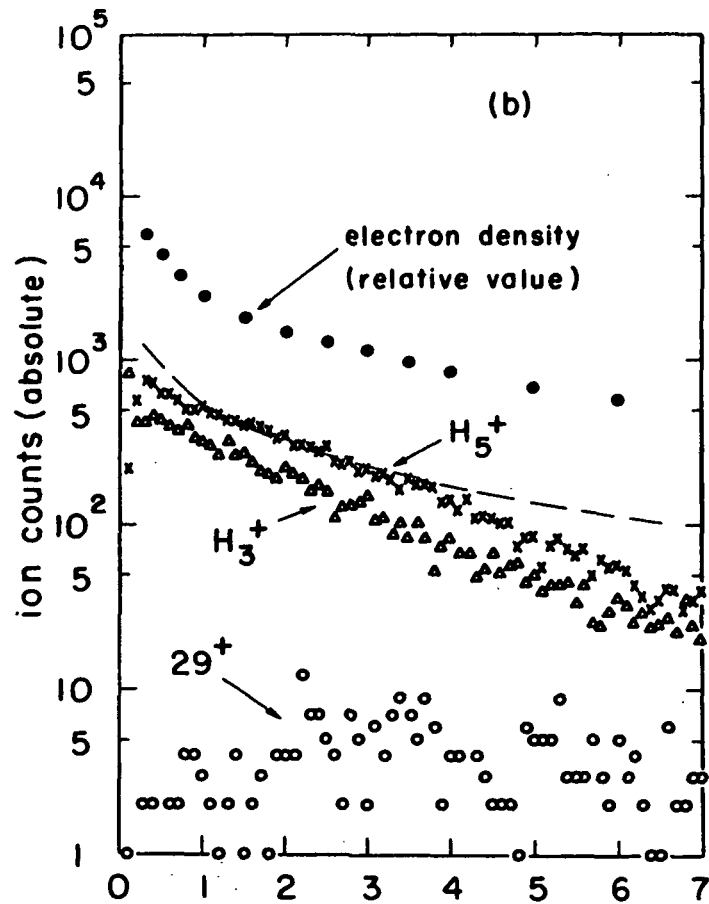
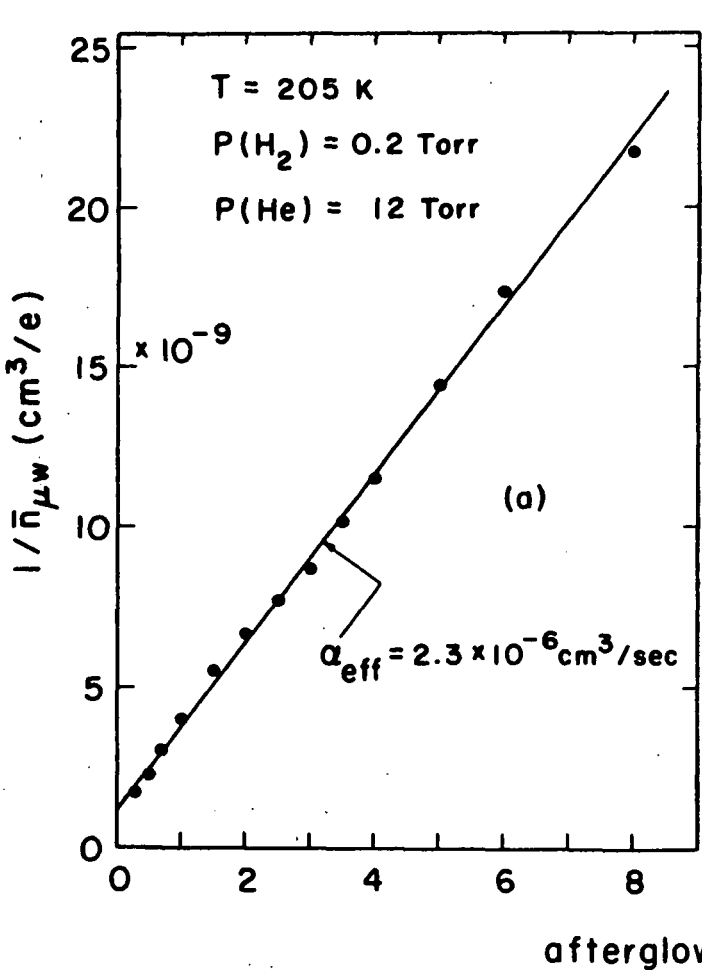


Figure 5

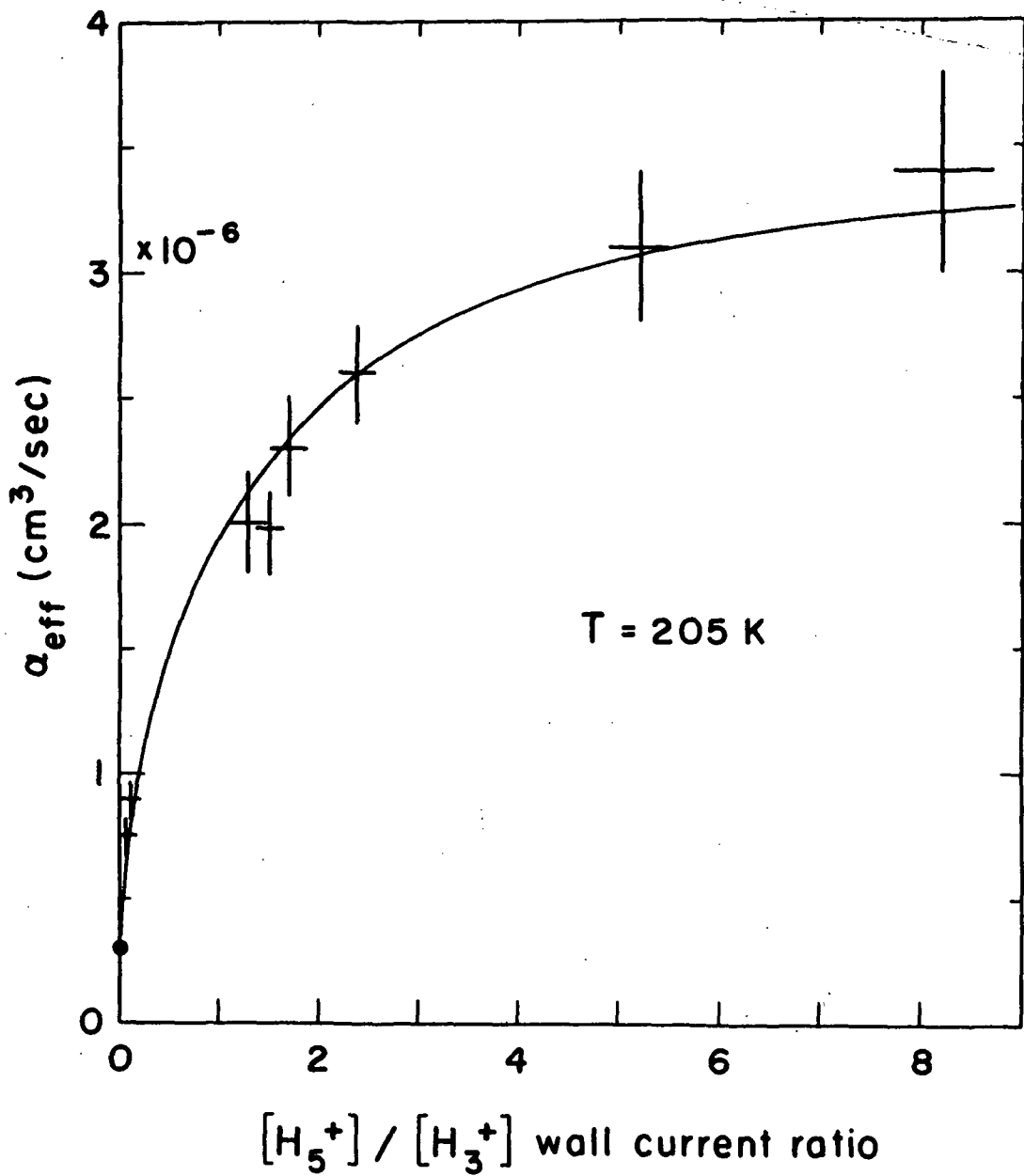


Figure 6

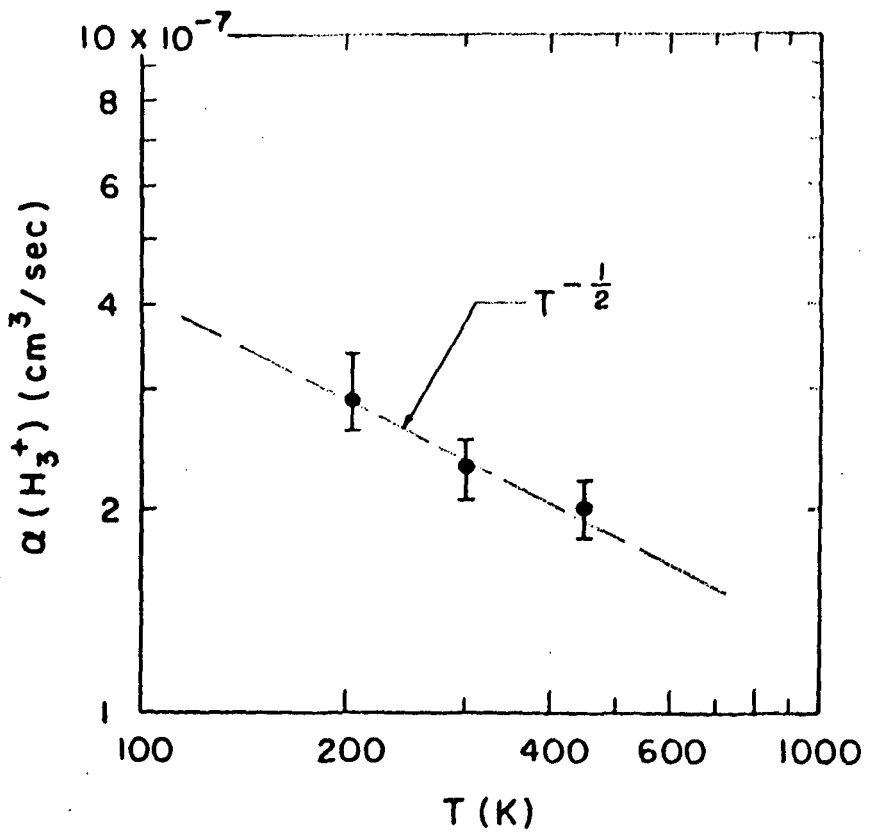


Figure 7